Atmos. Chem. Phys. Discuss., doi:10.5194/acp-2016-849, 2016
Manuscript under review for journal Atmos. Chem. Phys.
Published: 5 October 2016

Atmospheric Chemistry and Physics Discussions

The G4Foam Experiment: Global Climate Impacts of Regional Ocean Albedo Modification

Corey J. Gabriel*, Alan Robock, Lili Xia, and Brian Zambri

Department of Environmental Sciences, Rutgers University, New Brunswick, NJ, USA

Submitted to *Atmospheric Chemistry and Physics*
Special Issue: The Geoengineering Model Intercomparison Project

September, 2016

*To whom correspondence should be addressed: Corey J. Gabriel, Department of Environmental Sciences, Rutgers University. 14 College Farm Road. New Brunswick, NJ 08901-8551. E-mail: corey@envsci.rutgers.edu.

Atmos. Chem. Phys. Discuss., doi:10.5194/acp-2016-849, 2016
Manuscript under review for journal Atmos. Chem. Phys.
Published: 5 October 2016

Atmospheric Chemistry and Physics Discussions

Abstract. Reducing insolation has been proposed as a geoengineering response to global warming. Here we present the results of climate model simulations of a unique Geoengineering Model Intercomparison Project Testbed experiment to investigate the benefits and risks of a scheme that would brighten certain oceanic regions. The National Center for Atmospheric Research CESM-CAM4-CHEM global climate model was modified to simulate a scheme in which the albedo of the ocean surface is raised over the subtropical ocean gyres in the Southern Hemisphere. Like the commonly studied stratospheric geoengineering and marine cloud brightening proposals, this ocean albedo modification scheme is not currently possible. However, a stable, nondispersive foam, comprised of tiny, highly reflective microbubbles has been developed under idealized conditions, and, hence, a geoengineering scheme which simulates the effects of large-scale deployment of these microbubbles is appropriate to study at this time. One goal of this scheme is to cool Earth without reducing monsoon rainfall. We conducted three ensemble members of a simulation (G4Foam) from 2020 through 2069 in which the albedo of the ocean surface is raised to 0.15 over the three subtropical ocean gyres in the Southern Hemisphere, at the same time as increasing the radiative forcing with the RCP6.0 (representative concentration pathway resulting in +6 W m^{-2} radiative forcing by 2100) scenario, and then continuing the simulation for 20 more years with RCP6.0. Global mean surface temperature in G4Foam is 0.6 K lower than RCP6.0, with statistically significant cooling relative to RCP6.0 south of 30°N and an increase in rainfall over land, most pronouncedly in the tropics during the June-July-August season, relative to both G4SSA (specified stratospheric aerosols) and RCP6.0. Heavily populated and highly cultivated regions throughout the tropics, including the Sahel, Southern Asia, the Maritime Continent, Central America and much of the Amazon experience a statistically significant increase in precipitation minus evaporation. The temperature response to the relatively modest global average forcing of –1.5 W m^{-2} is amplified through a series of positive cloud feedbacks, in which more shortwave radiation is reflected. The precipitation response is primarily the result of the intensification of the southern Hadley cell, as its mean position migrates northward and away from the Equator in response to the asymmetric cooling.

Atmos. Chem. Phys. Discuss., doi:10.5194/acp-2016-849, 2016
Manuscript under review for journal Atmos. Chem. Phys.
Published: 5 October 2016

Atmospheric Chemistry and Physics Discussions

1 Introduction

1.1 Background

The current rate of increase in global mean surface temperature is unprecedented in the last 1,000 years (Marcott et al., 2013). This warming is co-occurring with a rate of increase in the atmospheric concentration of carbon dioxide (CO_2) and other greenhouse gases that exceeds any other increase in the recent record by one or two orders of magnitude, and the atmospheric concentration of CO_2 is higher now than at any time in the last 650,000 years (Siegenthaler et al., 2005). It is extremely likely that the warming since 1950 is primarily the result of anthropogenic emission of heat-trapping gases rather than natural climate variability (IPCC, 2013).

A global consensus on the need for mitigation has emerged as the December 2015 Paris Agreement at the 21st Conference of the Parties of the United Nations Framework Convention on Climate Change (UNFCCC). However, the UNFCCC lacks enforcement mechanisms, unlike the successful 1987 Montreal Protocol on Substances That Deplete the Ozone Layer, which legally obliged the signatories to phase out chlorofluorocarbons by 1998. Further, the Paris Agreement relies on nonbinding pledges from nations and avoids explicit emissions targets for specific countries. Our ability to reach the aspirations set out in the Paris Agreement will largely rely on these voluntary contributions to mitigation efforts. The nature of these voluntarily contributes are to be determined on the national level. Even then, attaining the Paris targets will likely require large-scale removal of carbon dioxide from the atmosphere (Fuss et al. 2014; Sanderson et al. 2016), which would require carbon dioxide removal to work as intended.

Therefore, even post-Paris, most realistic emission scenarios still send the global mean surface temperature to more than 2 K above preindustrial. Sophisticated adaptation efforts, including the planning of infrastructure projects in anticipation of an increase in extreme events, are underway (Miller et al., 2013; Fischbach et al., 2016). However, resources are finite and the planning of and execution of sophisticated large-scale projects necessary for adaptation has been largely limited to the world's richest countries.

Under these conditions, it is easy to see that the combination of mitigation and adaptation may be insufficient to spare us from progressively more disruptive impacts of global warming. This sad reality elevates the discussion of solar radiation management (SRM) geoengineering to relevance. SRM has been proposed as a method of reducing global mean temperature, thereby ameliorating many of the negative effects of global warming (Crutzen, 2006). The most discussed SRM approach involves injection of sulfur dioxide (SO_2) into the tropical stratosphere. The SO_2 reacts with water and aqueous sulfuric acid (H_2SO_4(aq)) is formed. It is theorized that this will then form a relatively stable layer of H_2SO_4(aq) droplets with a diameters of less than about 1 μm and mix globally through the Brewer-Dobson circulation, reflecting incoming shortwave (SW) radiation at all latitudes. Other suggested SRM geoengineering methods include marine cloud brightening (Jones et al., 2009; Rasch et al., 2009; Latham et al., 2010) and surface albedo modification (Irvine et al., 2010; Cvijanovic et al., 2015). Each of these methods has the potential to cool Earth's surface, but each comes with known potential side effects, many of which would be undesirable. For example, Robock (2008, 2014) enumerates and describes specific risks and benefits of stratospheric geoengineering.

Here we present a Geoengineering Model intercomparison Project (GeoMIP) testbed experiment (Kravitz et al., 2011, 2016), consisting of the novel implementation of an ocean surface albedo modification scheme in a climate model, which simulates the placement of a reflective foam, consisting of microbubbles, on the ocean surface. The albedo of the ocean surface is raised from a daily average 0.06 to a fixed daytime value of 0.15 over the subtropical

Atmos. Chem. Phys. Discuss., doi:10.5194/acp-2016-849, 2016
Manuscript under review for journal Atmos. Chem. Phys.
Published: 5 October 2016

Atmospheric Chemistry and Physics Discussions

ocean gyres in the Southern Hemisphere, specifically 20°N-20°S, 90°W-170°W (South Pacific), 20°N-20°S, 30°W-0°E (South Atlantic) and 20°N-20°S, 55°E-105°E (South Indian) (Fig. 1). This is the G4Foam experiment, which simulates a particular implementation of an idealized form of the technology described by Aziz et al. (2014), where stable, reflective foam suitable for use as SRM in ocean regions with limited nutrients that support little marine life is made in the laboratory.

The broad idea of microbubble deployment as a form of SRM is explored by Seitz (2010). Here we only examine the potential benefits and risks of such a scheme, and do not advocate deployment of any form of geoengineering even if it were presently possible. Robock (2011) has cautioned against the potential implications of ocean albedo modification as presented by Seitz (2010).

Stratospheric aerosol injections (SAI) are the most discussed, and given current state of research the most feasible, form of geoengineering (Dykema et al., 2014, Keith et al., 2014). Implementation of the G4Foam regional ocean albedo modification scheme could be considered with or without concurrent SAI. G4Foam could be used as a potential SSI concurrent scheme aimed at correcting possible negative impacts on the hydrological cycle brought about by ongoing SAI. G4Foam is also a potential alternative to SAI with a far different latitudinal distribution of benefits. The focus here is solely on the second scenario, as it allows for the elucidation of the impacts of the G4Foam experiment forcing alone.

While G4Foam and SAI are aimed in part at reducing surface temperature, their objectives vary in two profound ways. First, G4Foam primarily aims to enhance water supply by repositioning the tropical rain belts into highly populated, heavily cultivated areas. Second, unlike SSI, where the high latitude Northern Hemisphere (NH) cools preferentially, G4Foam preferentially cools Earth south of 30°N.

1.2 Motivation and Research Question

The goal of climate engineering is to reduce global warming without introducing additional risks. One of the major issues with stratospheric aerosols is a reduction of precipitation, especially for summer monsoons. The intervention discussed here attempts to reduce warming without reducing precipitation.

Is it possible to cool the planet while concurrently maintaining or increasing precipitation in highly populated and heavily cultivated regions, particularly in regions dependent on monsoon precipitation? We must begin by determining whether a forcing can be applied in a global climate model (GCM) that will result in the model responding with a northward and landward shift of tropical precipitation needed to achieve our objective. To that end we conducted simulations with The Community Earth System Model 1/Community Atmospheric Model 4 fully coupled to tropospheric and stratospheric chemistry (CESM1 CAM4–Chem) model (Lamarque et al., 2012; Tilmes et al., 2015, 2016). We ran the model with horizontal resolution of 0.9° x 1.25° lat-lon and 26 levels from the surface to about 40 km (3.5 mb), as was done for G4SSA (specified stratospheric aerosol) by Xia et al. (2016).

The experiments consisted of three ensemble members of a simulation from 2020-2089 in which the ocean surface albedo is raised as described above from a daytime average of 0.06 to a daytime constant 0.15 on the SH subtropical ocean gyres for 50 years, 2020-2069, and then returned to unforced values from 2070-2089 to assess termination. Our hypothesis is that the tropical rain belts will move northward largely as a result of increased moisture convergence over land regions, particularly during Northern Hemisphere (NH) summer (June-July-August, JJA) in NH monsoon regions. Enhanced divergence over the already strong subtropical highs,

Atmos. Chem. Phys. Discuss., doi:10.5194/acp-2016-849, 2016
Manuscript under review for journal Atmos. Chem. Phys.
Published: 5 October 2016

Atmospheric Chemistry and Physics Discussions

due to increased subsidence over the increased albedo ocean regions in the subtropical Southern Hemisphere (SH), would help the cooler air from the forced subtropical regions advect throughout the SH troposphere. The asymmetric cooling would force changes in the Hadley Cell, enhancing cross equatorial flow, which would cool the surface in the NH tropics, especially during JJA, when heat related mortality and morbidity is highest. Finally, the resulting cooling of low latitude NH land areas would not dampen the monsoon. The wet season monsoon circulation is initiated and maintained by the moist static energy gradient, not the surface temperature gradient. A wetter, more cloudy land mass will strengthen, not dampen the circulation relative to a warmer, drier continent (Hurley and Boos, 2014), especially with a cooler, lower specific humidity environment under the descending branch of the meridional circulation.

The strength of this response will be very sensitive to the cloud feedbacks that result from the surface albedo forcing. The basis of this comprehensive hypothesis is described in detail, below, specifically in sections 1.3 and 1.4. The details of the experiment are discussed in detail in section 2.

1.3 Stratospheric geoengineering weakens the hydrological cycle

With global warming, low-level specific humidity will increase by about 7% K^{-1} within the tropical planetary boundary layer. This response will be spatially homogeneous throughout the tropics. However, the precipitation response will be different. Increased moisture convergence in areas that already get a lot of precipitation will result in the "wet getting wetter," while increased moisture divergence in dry areas will result in the "dry getting drier" (Held and Soden, 2006).

The "rich get richer, poor get poorer" paradigm does not hold up in an SRM world, where the response is very different from that under global warming. Based on the results of an observational study, Trenberth and Dai (2007) pointed out the possibility that drought, particularly in the tropics, could result from geoengineering. This is based on a study of tropical volcanism, which provides a good analog to stratospheric SRM, particularly SSI approaches. They found that after the eruption of Mount Pinatubo (15°N) in 1991, precipitation dropped over land and record drops in runoff and river discharge were observed from October 1991 to September 1992.

Using a comprehensive atmosphere-ocean general circulation model, the National Aeronautics and Space Administration Goddard Institute for Space Studies ModelE, Robock et al. (2008) documented a reduction in rainfall over China and India, especially during NH summer, which is associated with a weakened monsoon. Changes in precipitation patterns also imply a southward shift of the intertropical convergence zone (ITCZ) over the Atlantic and Pacific Oceans. Additional similar experiments showed similar results.

In the GeoMIP G1 experiment, abrupt 4xCO2 forcing is applied to a year 1850 control climate, and the CO_2 forcing is fully offset by concurrent solar dimming (Kravitz et al., 2011). To explain the different hydrological cycle responses to surface and atmosphere energy balance responses to greenhouse gas and solar forcings, Kravitz et al. (2013) compared G1 with the experiment abrupt 4xCO2 and the Pre-Industrial Control experiment (picontrol), which is the reference experiment for both abrupt 4xCO2 and G1. They found a reduction in precipitation in G1 relative to abrupt 4xCO2 that can be separated into a fast component, due to the radiative response, which scales with the applied forcing, and a slow response, which is a temperature effect. Tilmes et al. (2013) analyzed the hydrological cycle in most of the GeoMIP participating Coupled Model Intercomparison Project 5 (CMIP5) (Taylor et al., 2012) models by comparing

Atmos. Chem. Phys. Discuss., doi:10.5194/acp-2016-849, 2016
Manuscript under review for journal Atmos. Chem. Phys.
Published: 5 October 2016

Atmospheric Chemistry and Physics Discussions

abrupt 4xCO2, picontrol, and G1. They found a robust reduction in global monsoon rainfall, including in the Asian and West African monsoon regions in G1 relative to both abrupt 4xCO2 and picontrol. Haywood et al. (2013) explored the impact of SSI in one hemisphere only and found a movement of the ITCZ away from the hemisphere that was cooler as a result of the asymmetric SSI.

This consensus about the potential for reduced tropical rainfall under a regime of stratospheric SRM motivates us to identify an alternative or SSI-adjunctive geoengineering approach that could cool the planet, without reducing monsoon precipitation in highly cultivated areas.

1.4 Extratropical forcing impacts the position of the ITCZ

Under global warming tropical rainbelts will move toward the hemisphere that warms more (Chiang and Bitz, 2005, Frierson and Hwang, 2012). Early atmosphere-ocean coupled models involved prescribed clouds. Increasing low cloud cover, and thereby inducing cooling, in one hemisphere relative to the other caused the tropical rainbelts over the Pacific Ocean to move toward the other hemisphere (Manabe and Stouffer, 1980). The impacts of asymmetric heating of the hemispheres became highly relevant during the Sahel drought. Much of the rainfall deficit during the devastating 20-30 year drought can be attributed to cooling initiated by increased tropospheric sulfate emissions in the NH (Hwang et al., 2013). The forced cooling over the NH was enhanced by a positive dynamical feedback in the North Atlantic Ocean. This hemispheric asymmetry moved Earth's energy flux equator, the vertical surface boundary where the vertically integrated meridional energy flux is zero, southward (Broccoli et al. 2006; Kang et al. 2008). Hence, the ITCZ and associated tropical rainbelts migrated south. Since the Sahel is at the northern margin of the ITCZs annual migration, or at the northern terminus of the West African monsoon, southward displacement of the ITCZ led to a devastating drought (Folland, 1986).

Broccoli et al. (2006) diagnosed the energy balance mechanism that causes the ITCZ to shift in response to asymmetric heating of the extratropics. Using models of varying complexity, Broccoli et al. (2006) imposed an anomalous cooling of the NH, either via a last glacial maximum simulation, or via hosing of the North Atlantic. The heating asymmetry causes the extratropics in the NH to demand more heat and the extratropics in the SH to demand less heat. Since cross equatorial heat transport is achieved principally via the Hadley Cell, the SH Hadley Cell strengthens, particularly in austral summer, in response to the NH cooling, and net energy flow in the upper branch intensifies, redistributing energy into the NH from the relatively warm SH.

Net flow of energy in the Hadley cell is achieved by the flow of moist static energy, which flows in the direction of the upper troposphere branch of the Hadley Cell. This is because moist static energy is higher at higher altitudes in the troposphere due to the increased contribution of the geopotential energy term overwhelming the moisture and internal energy terms in the moist static energy equation for the high altitude air. Net transport of energy, occurring in the upper branch of the Hadley cell from the SH to the NH, leads to increased moisture advection to the SH in the lower branch of the Hadley Cell. This redistribution of energy causes the ascending branch of the Hadley cell to migrate to the warmer SH where moisture convergence is increased and convective quasi-equilibrium is achieved under the relatively narrow poleward shifted ascending branch of the stronger SH winter Hadley Cell. This mechanism leads to the southward-displaced tropical rain belts (Broccoli et al., 2006).

This result is consistent with Lindzen and Hou (1988), who used a relatively simple model to show that even a small movement of maximum heating poleward into one hemisphere

Atmos. Chem. Phys. Discuss., doi:10.5194/acp-2016-849, 2016
Manuscript under review for journal Atmos. Chem. Phys.
Published: 5 October 2016

Atmospheric Chemistry and Physics Discussions

causes great asymmetry in the Hadley Cell, with the winter cell intensifying tremendously and the summer cell becoming rather modest. Further simplified model studies continued to elucidate the mechanism of extratropical forcing of the ITCZ. Kang et al. (2008) heated the SH poleward of 40°S while cooling the NH poleward of 40°N by an equal amount. The overall energy in the system was unchanged. The atmosphere was coupled to a simple swamp ocean. Interhemispheric heat exchange could only be achieved through the atmosphere. In this model, the energy flux equator and tropical rain bands moved to the SH.

In the real world, the ocean also plays a vital role in pushing the ITCZ into the warmer hemisphere. This is well-described by Xie and Philander (1994). They used a mixed layer ocean model, coupled with a simple atmosphere, which was capable of transporting momentum and heat to the ocean. This impacts SST via surface wind-induced mixing. Asymmetric heating produced a single ITCZ that forms in one hemisphere only. The atmosphere forced enhanced equatorial upwelling in the asymmetric Hadley Cell solution. This pushed the ITCZ toward warmer SSTs in the warmer hemisphere.

GCM results confirm this mechanism and connect the changes due to northward displacement of the ITCZ with the onset of active periods in the Asian summer monsoon (Chao and Chen 2001). It is evident that a geoengineering technique that could preferentially cool the SH could shift the tropical rain bands northward. However, in a GCM there are clouds. How would clouds respond in the hemisphere cooled by geoengineering? Would clouds change in the area being directly cooled? Would a cooling of the subtropics either directly, or indirectly via eddy flux from the artificially cool high latitudes, cause an increase in subtropical subsidence? Would this increase in the sinking of air above the intensified subtropical highs cause water vapor to be trapped in the lower troposphere, forming low clouds and suppressing water vapor mixing into the free troposphere, where the water vapor may instead be used up in formation of high clouds, which tend to reduce outgoing longwave radiation? Informed by these established diagnostic mechanisms associated with the impacts of asymmetric heating of the hemispheres, we seek to concurrently cool the entire SH and the NH tropics, modestly cool the NH extratropics and, most importantly, induce an anomalous overturning circulation and redistribute rainfall from ocean to land and from south to north across the tropics.

2. Methods

2.1 Design of experiment and model configuration

Figure 1 shows the regions selected for albedo enhancement. These regions were chosen because of their low cloud fraction, low wind speeds, weak currents, and lack of biological productivity in addition to the likelihood that the surface cooling in this area will advect well within the SH.

We used the Community Land Model (CLM) version 4.0 with prescribed satellite phenology (CLM4SP) instead of the version of CLM with a carbon–nitrogen cycle, coupled with CAM4–chem. Vegetation photosynthesis is calculated under the assumption of prescribed phenology and no explicit nutrient limitations (Bonan et al., 2011, Xia et al., 2016). Dynamic vegetation is not turned on in this study. The ocean model does not include any biogeochemical responses.

The fundamental question we wish to answer concerns representation of the physical processes that lead to realistic simulation tropical precipitation. The Asian monsoon is of great importance in that investigation. Fortunately, monsoon processes and regimes are depicted well in our atmospheric component, CAM4 (Meehl et al., 2012). Some important features of CAM4 that illustrate its very good monsoon representation include the amount and location of

Atmos. Chem. Phys. Discuss., doi:10.5194/acp-2016-849, 2016
Manuscript under review for journal Atmos. Chem. Phys.
Published: 5 October 2016

Atmospheric Chemistry and Physics Discussions

precipitation over the southern Tibetan Plateau and over the Western Ghats (a mountain range near the west coast of south India). This is improved when compared to earlier versions of the model. The rain shadow leeward of this range is often not resolved by GCMs, however CAM4 shows some evidence of this rain shadow. These changes related to orography and horizontal resolution are important and likely generalize to similar land surface features outside of India, where model biases have not been as carefully studied as they have been in heavily populated southern India. This improvement can be attributed to the CCSM4 finite-volume dynamical core, which replaces the spectral version of the CCSM3 and the interconnected higher horizontal resolution. Additionally, large-scale features are improved. For example, the representation of the ITCZ during NH winter southward migration over the maritime continent is improved (Meehl et al., 2011).

There is an important process associated with monsoon precipitation, however, that is pervasively wrong across CMIP5. Zonal mean absorbed shortwave radiation is too high over the southern ocean (Kay et al., 2016). This cloud problem leads to a warmer Southern Ocean, which leads to anomalous SH atmospheric eddy flux to the subtropics from the extratropics, potentially damping the cooling response of our negative surface radiative forcing in the subtropical oceans. The effect of a transfer of heat from the SH extratropics into the Hadley Cell already causes a relatively weak negative bias in the amount of interhemispheric heat transport from the south to north. Therefore, the manifestation of this bias in G4Foam would be to partially offset our imposed cooling, lessening the need for interhemispheric energy transport to the SH and suppressing the surface return flow of moisture advection into the NH. Lower than observed interhemispheric energy transport would be associated with a weaker Asian monsoon. However, this feature is equally present in our G4Foam experiment and its control experiments so will not affect the differences.

We compare G4Foam to two control experiments. First is a specific sulfate injection scenario, G4 Specified Stratospheric Aerosol (G4SSA; Xia et al., 2016). They used a prescribed stratospheric aerosol distribution roughly analogous to annual tropical emission into the stratosphere (at 60 mb) of 8 Tg SO_2 yr^{-1} from 2020 to 2070. This produces a radiative forcing of about −2.5 W m^{-2}. The G4SSA forcing ramps down from 2069-2071 and then continues without additional forcing from 2072-2089. In G4SSA tropospheric aerosols are not affected by the prescribed stratospheric aerosols. Therefore we cannot evaluate how stratospheric aerosols would actually fall out and impact the chemistry, dynamics and thermodynamics of the troposphere from this experiment. Neely et al. (2015) offers more detail on the prescription of stratospheric aerosols in CAM4–Chem. The second control, which serves as the reference simulation, for both G4Foam and G4SSA is the Representative Concentration Pathway 6.0 (RCP6.0) (Meinshausen et al., 2011) from 2004 to 2089. We have run three ensemble members each for G4Foam, G4SSA, and RCP6.0.

2.2 Ocean albedo enhancement approach

The advent of a plausible technology to make quantities of long lasting foam, or engineered microbubbles to enhance ocean albedo, elevates ocean albedo modification to a status of plausibility that is roughly equivalent to that of other widely discussed potential geoengineering methods. Seitz (2010) speculated that since air-water and air-sea interfaces are similarly refractive, dispersing microbubbles onto the surface of the ocean would reflect sunlight in much the same way as cloud droplets do. While engineering refractive or stable foams is commonly done and applied in both food science and firefighting, engineering a stable and refractive foam appropriate for a geoengineering scheme appeared fanciful until Aziz et al.

Atmos. Chem. Phys. Discuss., doi:10.5194/acp-2016-849, 2016
Manuscript under review for journal Atmos. Chem. Phys.
Published: 5 October 2016

Atmospheric Chemistry and Physics Discussions

(2014) produced a long lasting refractive foam made with biodegradable and non-toxic additives. Aziz et al. identified foam lifetime of three months or more per microbubble as lasting long enough that the input of energy to create the microbubbles would not be prohibitive. After experimenting with protein-only solutions, Aziz et al. (2014) added "high methyl ester pectin to type A gelatin" and created a foam in salt water, which was still intact and stable at the cessation of the experiment after 3 months. The reflectance of the foam was about 50%, which is comparable to that of whitecaps. The creation of these stable microbubbles makes enhancing ocean albedo in this manner "feasible" (Aziz et al. 2014).

Safe, stable, highly reflective microbubbles were created in saltwater in a laboratory. However, this technology – like other SRM techniques – is still a long way from deployment. For example, what effect would bacteria in the ocean have on the surfactant? There are a number of other potential risks associated with microbubble deployment, even if the feasibility issues are set aside. Robock (2011) pointed out that vertical mixing in the ocean, changes in ocean circulation, impacts on photosynthesis, and risks to the biosphere could all impair the efficacy of this geoengineering approach. Robock (2011) also pointed out that a cooler ocean would serve as a more effective CO_2 sink, helping to offset the CO_2 increase that comes about as a feedback of warming. Other potentially attractive attributes of this technique include the possibility that it could be deployed exclusively in the 20% of the world's oceans that are not biologically active (Aziz et al. 2014) and therefore have little impact on the biosphere, that there would be no risk to ozone in the stratosphere.

3 Results

The following results compare the G4Foam climate with the climates in G4SSA and RCP6.0 averaged over the period 2030-2069. While G4Foam and G4SSA forcing commences in 2020, the first ten years of both experiments are a period of transition. For that reason 2020-2029 is discarded from our comparisons.

3.1 Temperature and cloud response

The primary purpose of G4Foam is to reduce global mean surface temperature without reducing monsoon precipitation. G4Foam would reduce global mean surface temperature relative to RCP6.0 by 0.60 K and global mean land surface temperature by 0.51 K relative to RCP6.0. In JJA, G4Foam is 0.70 K cooler than RCP6.0 over land in the tropics, 20°S-20°N. (Table 1). This JJA cooling in the tropics is of particular importance due to the dense population and heavy agricultural demand in the tropics, particularly north of the equator. The G4Foam cooling is achieved by a change in net clear sky top of atmosphere flux in G4Foam of –1.5 W m^{-2} (Figure 2).

G4Foam does not achieve the same amount of cooling as G4SSA, which would reduce global mean surface temperature by 0.92 K. This is achieved by a change in net clear sky top of atmosphere shortwave flux in G4Foam of –4.0 W m^{-2}. On a global mean basis and relative to RCP6.0, G4Foam achieves 66% of the cooling produced by G4SSA, while applying only 38% as much forcing as G4SSA (Figure 2). This implies that much of the G4Foam cooling is the result of positive feedbacks, which enhance the cooling, as discussed below.

Figure 3 shows a comparison of the spatial distribution of surface temperature changes between G4Foam and G4SSA and between G4Foam and RCP6.0 between 2030-2069. Over the SH ocean gyres that were brightened (Fig. 1), we see a very robust cooling, reaching 2 K at the center of the South Pacific foamed region. However, the cooling mixes rather well throughout the SH. Cross equatorial flow and changes in the Hadley Cell transmit this cooling into the NH

Atmos. Chem. Phys. Discuss., doi:10.5194/acp-2016-849, 2016
Manuscript under review for journal Atmos. Chem. Phys.
Published: 5 October 2016

Atmospheric Chemistry and Physics Discussions

tropics through the mechanisms described in section 1.4, above. Some of this cooling in the NH tropics is then transmitted to the NH extratropics.

G4Foam is significantly cooler ($p < 0.05$) than RCP6.0 in almost all locations south of 30°N, in mid latitude NH continental regions windward of the Atlantic and Pacific, and at very high latitudes. Figure 3d shows that G4Foam is less effective in cooling extratropical NH land regions during JJA. This is reasonable, since continental heating in the NH JJA season is more dominated by local heating than the other seasons, in which meridional energy transport plays a larger role. Figures 3a and 3c show that G4SSA is more effective over NH continents than G4Foam. A key weakness of G4Foam, if implemented alone, would be its failure to adequately reduce human suffering induced by heat stress in NH mid-latitudes during the summer as a result of ongoing global warming.

Since the G4Foam forcing alone, with the amplitude of the current experiments, would be insufficient to achieve any of the objectives of the G4Foam experiment, positive feedbacks that enhance cooling and circulation responses must be triggered by the G4Foam forcing to enhance a resulting cooler, wetter climate. Figure 4 shows change in low cloud fraction both year-round and in the JJA season. The largest change is in the northern half of the regions where foam is applied, and the area to the north of those foamed regions. The changes in low clouds in these regions are both large and statistically significant. We attribute much of this low cloud response to prevailing southeasterly winds in the SH tropics advecting cold air northeastward, through the northern part of the foamed regions and then over the warmer tropical waters equatorward of the foamed regions. This cold advection over relatively warm water forms broad regions of low clouds in these subtropical and tropical regions (Fig. 4).

Another striking G4Foam feature is the large and statistically significant increase in low clouds over land across central Africa, the Middle East and Southeast Asia. These low clouds are coincident with the large cooling in Africa and the Middle East, particularly during the JJA season relative to both G4SSA and RCP6.0 (Figs. 4c, 4d). These are very hot areas and heat related mortality and morbidity are of great concern. A similar increase in low clouds is evident in the tropical eastern Pacific. This is coincident with the mean northward displacement of the ITCZ in G4Foam with respect to G4SSA and RCP6.0, not with any changes in the El Niño-Southern Oscillation (ENSO).

In G4Foam, clouds are the key to changing the radiation budget in the tropics. In G4Foam there is a change in shortwave cloud forcing of –2.32 W m^{-2} annually and –2.59 W m^{-2} during JJA, relative to G4SSA. Only very small increases in longwave cloud forcing of 0.42 W m^{-2} annually, and 0.07 W m^{-2} in JJA counter this negative forcing. The overall change in cloud radiative forcing in the tropics is –1.90 W m^{-2} annually and –2.52 W m^{-2} during JJA.

Total cloud fraction is shown in Fig. 5. Figs. 5c and 5d are particularly striking in showing the increase in clouds over Africa and Southeast Asia during the JJA wet monsoon season in those regions. Under G4Foam, these regions generally experience cloudier and cooler summers relative to RCP6.0 and are cloudier and only very slightly warmer on average compared to G4SSA. Some parts of the Sahel and the Middle East are actually slightly cooler in G4Foam than RCP6.0. These changes in temperature and cloudiness play a key role in the changes in the hydrological cycle under G4Foam, which we discuss next.

3.2 Hydrological Cycle Response

Relative to G4SSA, precipitation in G4Foam over land in the tropics increases by 3.9% on an annual mean basis and by 4.9% during JJA (Table 1). Tropical precipitation in G4Foam over land in the tropics increases by 1.4% on an annual mean basis and by 2.02% during JJA,

Atmos. Chem. Phys. Discuss., doi:10.5194/acp-2016-849, 2016
Manuscript under review for journal Atmos. Chem. Phys.
Published: 5 October 2016

Atmospheric Chemistry and Physics Discussions

when compared to G4SSA. Each of these changes is statistically significant ($p < 0.05$). Regarding the temperature change relative to G4SSA, G4Foam is only about 0.3 K warmer in the tropics. The temperature dependence of precipitation, between 1.5% K^{-1} and 3.0% K^{-1}, (Emori and Brown, 2005), explains only a fraction of the precipitation increase. The statistically significant increase in land-only precipitation in the tropics in G4Foam relative to RCP6.0 occurs in a climate in which RCP6.0 is between 0.6 K and 0.7 K warmer than G4Foam, depending on the season. Over the tropical oceans, in G4Foam, precipitation only increases by 0.8% on an annual mean basis and 0.7% during JJA relative to G4SSA and there is a decrease of 1.6% on an annual mean basis and a decrease of 1.9% during JJA relative to RCP6.0. These changes imply that there is a large increase in moisture convergence over land in the tropics in G4Foam relative to both G4SSA and RCP6.0.

Globally, over land, the response is similar, but the magnitude of change is a bit less. Precipitation is statistically significantly increased over land in G4Foam relative to RCP6.0 by about 0.5%. Precipitation is statistically significantly increased in G4Foam relative to G4SSA over land by 3.5%.

The overall global precipitation difference between G4Foam and G4SSA or RCP6.0 when land and ocean are combined and all seasons and all latitudes are included are in line with the magnitude of the temperature dependence of precipitation. Globally, G4Foam is warmer than G4SSA by 0.3 K and there is 0.61% more precipitation. G4Foam is cooler than RCP6.0 by 0.6 K and drier by 1.98%.

The spatial pattern of precipitation changes is shown in Fig. 6. Precipitation is greatly reduced over the ocean, particularly in the SH, relative to both G4SSA and RCP6.0. Changes in precipitation poleward of 40° latitude in either hemisphere are largely due to the temperature dependence of precipitation. The changes in the SH subtropics are dominated by the shortwave forcing applied over the ocean gyres, which reduces both evaporation and precipitation in those areas.

The changes in precipitation in the tropics are driven by the ITCZs northward shift. Large precipitation anomalies occur in a narrow band north of the equator and smaller positive anomalies occur in broader regions, primarily over NH monsoon regions. Importantly, we see a statistically significant increase in monsoon precipitation over the Sahel, the Middle East, the Indian subcontinent as well as southwest Asia and the maritime continent on an annual mean basis in G4Foam relative to G4SSA (Figure 6a). Relative to RCP6.0, these changes are not statistically significant over the Indian subcontinent or southwest Asia, but there are only very isolated and small areas in these regions in which there is any precipitation reduction, either on the annual mean or during JJA. Therefore, over much of heavily populated southern Asia, east of the Arabian Sea, G4Foam will be cooler than RCP6.0 without any notable precipitation differences.

Relative to both G4SSA and RCP6.0, there is a great deal more precipitation all year and particularly during JJA over central America, the northern Amazon, much of Africa, parts of the Arabian peninsula and the maritime continent. This response is more robust than the response over Southeast Asia due to the more direct dependence of rainfall in these regions on ITCZ position than in Southeast Asia, where the monsoon is also driven by numerous local and remote factors, including ENSO and the Indian Ocean Dipole.

Although these G4Foam simulations are effective in enhancing moisture convergence over heavily populated and highly cultivated regions, particularly in the tropics, there are regions that would suffer under this regime. Precipitation patterns for islands in the South Pacific are

Atmos. Chem. Phys. Discuss., doi:10.5194/acp-2016-849, 2016
Manuscript under review for journal Atmos. Chem. Phys.
Published: 5 October 2016

Atmospheric Chemistry and Physics Discussions

largely governed by the position and strength of the South Pacific Convergence Zone (SPCZ), which changes substantially under G4Foam due in part to the cooling and to the movement of gradients of temperature and pressure. Precipitation deficits over Madagascar and some regions in Africa and South America exceed 10%. However, the very large precipitation deficits in G4Foam are largely confined to the SH oceans and the land areas that tend to be far less populated than in the areas where it will increase.

While the changes in precipitation are important and useful in describing the climate response in G4Foam, the change in precipitation minus evaporation between G4Foam and G4SSA or RCP6.0 is more relevant to how the changes in climate will actually impact people's lives. Figure 7 shows precipitation minus evaporation. Specifically Fig. 7a shows that precipitation minus evaporation in G4Foam is increased, and this increase is significant relative to G4SSA, across the Sahel, all of South Asia, the Maritime Continent, Central America and the northern Amazon. These are all heavily populated regions that are heavily cultivated. Figure 7b shows a similar pattern, albeit with the regions significantly gaining water slightly suppressed in coverage, when G4Foam is compared to the warmer RCP6.0 rather than G4SSA. Figures 7c and 7d show changes in water supply during JJA, the NH wet monsoon season, when water is likely needed the most. Due to variability in the monsoon, there is more heterogeneity in the JJA response than the annual response, particularly across Southeast Asia. The water gain, driven by a combination of increased precipitation, lower temperature and increased cloudiness in these heavily cultivated regions, is the most important benefit of G4Foam.

Figure 8 shows the differences of annual cycles from 2030-2069 for zonal mean precipitation, zonal mean precipitation minus evaporation, and zonal mean precipitable water between G4Foam and G4SSA and between G4Foam and RCP6.0. They illustrate the northward displacement of the ITCZ, with positive precipitation anomalies progressing poleward as the boreal summer monsoon progresses. Figure 8f shows the difference in the zonal mean annual cycle for column integrated precipitable water between G4Foam and RCP6.0. The striking feature here is that zonal mean precipitation is higher at key latitudes in the tropics, despite zonal mean column integrated precipitable water being much lower at the same latitude. This further illustrates the presence of increased moisture convergence further north, at latitudes with more land and population, which explains the precipitation increase concurrent with the decrease in available water vapor.

In Fig. 9, we quantify the impacts on agriculture by looking at the photosynthesis rate anomalies between G4Foam and RCP6.0. There are small, but statistically significant increases, in photosynthesis rate in G4Foam relative to RCP6.0 in much of Southeast Asia. The most dramatic changes occur in Central America and parts of the northern Amazon, where the high CO_2, relatively cool and very wet conditions promote agriculture.

4 Discussion

This paper is an analysis of a geoengineering climate model experiment. Although for this experiment, global warming is reduced without negative impacts on precipitation, as was found in previous stratospheric aerosol implementations, this does not argue for the implementation of climate engineering. Any such decisions will need to balance all the risks and benefits of such implementation, and compare them to those from other possible responses to global warming.

4.1 Summary

G4Foam would reduce global mean surface temperature relative to RCP6.0 by 0.6 K for the 40-year period starting 10 years after the implementation of geoengineering. Clear sky top of

Atmos. Chem. Phys. Discuss., doi:10.5194/acp-2016-849, 2016
Manuscript under review for journal Atmos. Chem. Phys.
Published: 5 October 2016

Atmospheric Chemistry and Physics Discussions

atmosphere net shortwave flux is reduced by 1.5 W m^{-2} in G4Foam relative to RCP6.0. This is achieved primarily by the shortwave forcing over the subtropical SH ocean gyres. Before accounting for feedbacks, temperature is more sensitive to the forcing applied in G4Foam than G4SSA. However, global mean surface temperature in G4SSA 0.3 K lower than G4Foam because of a larger change in clear sky top of atmosphere net shortwave flux of –4.0 W m^{-2} (Fig. 2). Additionally, the latitudinal distribution of temperature reduction is different in G4Foam than in G4SSA. G4SSA is most effective in cooling the NH continents, while G4Foam most effectively cools the surface south of around 30°N (Fig. 3). Precipitation over land globally, in the tropics, during JJA globally, and during JJA in the tropics is statistically significantly increased in G4Foam relative to both G4SSA and RCP6.0 (Fig. 6). The combination of cooling and increased precipitation over land in the tropics results in a statistically significant increase in precipitation minus evaporation on an annual mean basis over Central America, the Northern Amazon, the Sahel, the Indian Subcontinent, the Maritime Continent and Southeast Asia in G4Foam relative to G4SSA (Fig. 7). All of these areas are very densely populated and heavily cultivated. Water scarcity is a major issue in these areas and G4Foam describes a climate model response in which there is global cooling but more water is made available to many people in regions on the brink of severe water shortages. Both the changes in the spatial pattern and magnitude of changes in temperature and precipitation are far too large to be explained by the forcing alone. Instead, much of the temperature and hydrological response is the result of powerful cloud feedbacks and changes in the tropical meridional overturning circulation induced by the placement of the ocean albedo forcing.

4.2 The hydrological response

The dominant cause of the G4Foam hydrological response is the intensification of the southern Hadley Cell and the northward migration of the ITCZ in response to the asymmetric forcing. However, the precipitation response is not zonally homogeneous, as the regional and local mechanisms are also important to the distribution of precipitation.

First, we address the increase in precipitation over Central America. For this, we turn to literature concerning the decline of Mayan civilization in Central America. Summer insolation in the NH began to decrease about 5,000 years ago. The ITCZ migrated southward. This southward shift caused rainfall to decrease in the crucial summer growing season. Long droughts and eventually water shortages contributed to the civilization's decline (Poore et al., 2004). In G4Foam, the ITCZ moves northward and the areas in which Mayan civilization flourished, including Belize, Guatemala and parts of Mexico, once again receive a great deal more precipitation. This response is incredibly strong and consistent in each ensemble member (Figs. 6-8).

The long mid-to-late 20th century Sahel drought was primarily caused by the ITCZ being pushed southward by preferential cooling of the NH (Folland, 1986). In G4Foam, the reverse is true. SH cooling pushes the ITCZ north, which generally explains the G4Foam precipitation increase in the Sahel.

A surprising finding is that portions of the Arabian Peninsula equatorward of 20°S experience precipitation increases of up to 1 mm day^{-1} during the JJA season. However, this northward migration of boreal summer precipitation is evident in the paleoclimate record. Evidence of such precipitation is found in Fleitmann et al. (2003), who showed changes in $\delta^{18}O$ in cave stalagmites in Oman, which indicate increased rainfall in Oman under the influence of northward movement of the ITCZ over the Indian Ocean in periods of relative warmth in the NH relative to the SH.

Atmos. Chem. Phys. Discuss., doi:10.5194/acp-2016-849, 2016
Manuscript under review for journal Atmos. Chem. Phys.
Published: 5 October 2016

Atmospheric Chemistry and Physics Discussions

Changes in precipitation over the Maritime Continent are partially attributable to large-scale convergence and rising air in those regions, as they lie longitudinally between G4Foam forcing zones where subsidence is enhanced. However, the Indian Ocean Dipole (IOD) (Cai et al., 2012; Chowadry et al., 2012) and Subtropical Indian Ocean Dipole (SIOD) phenomena discussed below are more likely the key drivers of the precipitation response over the Maritime continent.

In its positive phase, the SIOD features anomalously warm SSTs in the southwestern Indian Ocean, east and southeast of Madagascar, and cold anomalies of SST west of Australia. Stronger winds prevail along the eastern edge of the SH subtropical high over the Indian Ocean, which becomes intensified and shifted slightly to the south during positive SIOD events. This results in more evaporation over the eastern Indian Ocean, which cools SSTs in the Indian Ocean east of Australia (Suzuki et al., 2004). In the SIOD negative phase, the opposite is $_{\text{true}}$. There is cooler water in the southwest Indian Ocean, near Madagascar and warmer waters to the east, near Australia (Behera et al., 2001; Reason, 2001).

The negative phase of the SIOD features more precipitation in western Australia and the Maritime Continent. This negative SIOD phase is consistent with the SST pattern in the Indian Ocean forced by G4Foam. Therefore, the negative SIOD like mean state in G4Foam appears to play a role in the enhanced rainfall in Northwestern Australia and the Maritime Continent.

Based on both local and global changes in circulation, we expected a very large increase in the strength of the Indian Monsoon. In addition to the planetary scale changes associated with the ITCZ and the Hadley cell, the position of the semi-permanent high in the subtropical Southern Indian Ocean also plays a large role in modulating the Indian summer monsoon. Negative SIOD events during boreal winter are often followed by strong Indian summer monsoons. During a negative SIOD event, the subtropical high in the Indian Ocean shifts northeastward as the season shifts from December, January, and February to JJA. This causes a strengthening of the monsoon circulation, intensifying the Hadley Cell locally during the JJA monsoon.

A negative IOD is associated with a weakened Asian monsoon and an increase in precipitation over Australia and the Maritime Continent. In G4Foam, advection of cold water in the Somali current into the equatorial western Indian Ocean creates a negative IOD-like response that partially counters the combination of the global scale Hadley cell response and the forced SIOD, dampening the overall increase in the Indian monsoon. This warm west, cold east mean state in the equatorial Indian Ocean resembles a negative IOD mean state and it helps to explain the enhanced precipitation response in the Maritime Continent and the lower than expected increase in precipitation over the Indian subcontinent. The Asian monsoon and precipitation over the Maritime Continent are also governed in part by ENSO. However, no changes in ENSO were evident in G4Foam relative to G4SSA or RCP6.0. There is also no evident response of ENSO amplitude or frequency to any of several different regimes of stratospheric geoengineering (Gabriel and Robock, 2015).

4.3 Caveats

The technology does not presently exist to actually deploy a stable, highly reflective layer of microbubbles on the actual ocean surface. While a stable, highly reflective, nondispersive foam has been developed in a saltwater solution, appropriate for climate engineering, this foam has not been tested outside the laboratory, much less on the surface of a large area of rarely quiescent ocean. The foam has not been immersed in a medium in which bacteria are present, and the interaction between the bacteria and the protein surfactant could damage the layer of

Atmos. Chem. Phys. Discuss., doi:10.5194/acp-2016-849, 2016
Manuscript under review for journal Atmos. Chem. Phys.
Published: 5 October 2016

Atmospheric Chemistry and Physics Discussions

microbubbles. Also, even though the diameter of these microbubbles is on the order of 10^{-6} m, the demand for surfactant would likely overwhelm our current production capacity of whatever surfactant is chosen. The research on the engineering required to perform stratospheric geoengineering by sulfate injection is much further along than research of microbubble deployment, which is still in its earliest stages.

However, since development of microbubble technology is underway, it is worthwhile to determine how such a technology could be applied in a manner that would address serious climate issues. The progress being made in research associated with stratospheric geoengineering actually enhances the relevance of researching the climate impact of this particular ocean surface geoengineering approach as G4Foam was designed with an eye toward concurrent deployment with stratospheric geoengineering in the event the stratospheric geoengineering were to cause the precipitation deficits that many model studies have shown that it might.

More fundamentally, the propriety of any attempt to impose a the G4Foam forcing in an attempt to achieve the modeled G4Foam climate is premised on a value judgment that it is desirable to develop a technology that could redistribute essential resources between nations in an attempt to achieve a net benefit to humanity as a collective when it unknowingly creates a local scarcity of these essential resources. To some extent, making this value judgment is germane and is a prerequisite to the discussion of any form of geoengineering. Even though G4Foam would be successful in increasing water supply in more heavily populated areas, water supply will almost certainly be reduced in remote regions, such as South Pacific islands. Is it ethical to pick winners and losers when the selection process is aimed at increasing the number of winners and decreasing the number of losers? Hypothetically, if G4Foam worked as described in this paper, from a purely consequentialist perspective, and with the sole objective being increased utility for the human collective, G4Foam could be considered beneficial.

Finally, this paper is concerned with the climate response to surface albedo changes. We do not examine how placing an actual layer of microbubbles in the ocean would change ocean circulation or impact chemistry and biology in the ocean. Evaluating the changes in the ocean, especially changes in its circulation that are caused by the surface albedo modification, is one of the next issues to explore. The ocean regions we propose to brighten have low biological productivity and weak currents, but the possibility of remote impacts, due to changes in circulation having negative impacts on important ocean regions, is worth considering.

4.4 Future research

Whether or not a concurrent deployment of stratospheric geoengineering and ocean albedo modification could cool the entire planet while maintaining or enhancing the hydrological cycle, particularly in the tropics, is the next natural step in this research. Such research is motivated by the need to determine whether some combination of geoengineering techniques can be used to offset undesirable regional climate disparities that using one method of geoengineering alone could induce.

Acknowledgments. This work is supported by U.S. National Science Foundation (NSF) grants AGS-1157525, GEO-1240507, and AGS-1617844. Computer simulations were conducted on the National Center for Atmospheric Research (NCAR) Yellowstone supercomputer. NCAR is funded by NSF. The CESM project is supported by NSF and the Office of Science (BER) of the U.S. Department of Energy.

Atmos. Chem. Phys. Discuss., doi:10.5194/acp-2016-849, 2016
Manuscript under review for journal Atmos. Chem. Phys.
Published: 5 October 2016

Atmospheric Chemistry and Physics Discussions

References

Aziz, A., Hailes, H.C., Ward, J.M. and Evans, J.R.G.: Long-term stabilization reflective foams in seawater. Royal Society of Chemistry. 95, 53028–53036. 2014.

Behera, S. K. and Yamagata, T.: Subtropical SST dipole events in the southern Indian Ocean, Geophysical Research Letters 28: 327–330, 2001

Bonan, G. B., Lawrence, P. J., Oleson, K. W., Levis, S., Jung, M., Reichstein, M., Lawrence, D. M., and Swenson, S. C.: Improving canopy processes in the Community Land Model version 4 (CLM4) using global flux fields empirically inferred from FLUXNET data, J. Geophys. Res., 116, G02014, doi:10.1029/2010JG001593, 2011.

Broccoli, A. J., Dahl, K. A. and Stouffer, R.J.: The response of the ITCZ to Northern Hemisphere cooling. Geophys. Res. Lett., 33, L01702, doi:10.1029/2005GL024546, 2006.

Cai W., Van Rensch P., Cowan T. and Hendon H.H.: Teleconnection pathways for ENSO and the IOD and the mechanism for impacts on Australian rainfall, J. Climate, 24:3910–3923, doi:10.1175/2011JCLI4129.1, 2011.

Chao, W.C. and Chen, B.: The origin of the monsoons, J. Atmos. Sci., 58, 3497–3507. 2001.

Chiang, J. C. H. and Bitz, C. M. Influence of high latitude ice cover on the marine Intertropical Convergence Zone. Climate Dynamics 25, 477–496, 2005.

Chowdary J.S., Xie, S-P, Tokinaga, H., Okumura, Y.M., Kubota H., Johnson N. and Zheng X-T: Interdecadal variations in ENSO teleconnection to the Indo–western Pacific for 1870–2007, J. Climate, 25:1722–1744. doi:10.1175/JCLI-D-11-00070.1, 2012.

Cvijanovic, I., Caldeira, K., and MacMartin, D.G.: Impacts of ocean albedo alteration on Arctic sea ice restoration and Northern Hemisphere climate, Environmental Research Letters, 10, 044020, doi:10.1088/1748-9326/10/4/044020, 2015.

Emori, S. and Brown, S.J.: Dynamic and thermodynamic changes in mean and extreme precipitation under changed climate, Geophysical Research Letters, 321,17, doi: 10.1029/2005GL023272, 2005.

Crutzen, P.: Albedo enhancement by stratospheric sulfur injections: A contribution to solve a policy dilemma?, Climatic Change, 77, 211–219, 2006.

Dykema J.A., Keith D.W., Anderson J.G., Weisenstein, D.: Stratospheric controlled perturbation experiment: a small-scale experiment to improve understanding of the risks of solar geoengineering, Phil. Trans. R. Soc. A 372, 20140059, doi:10.1098/rsta.2014.0059, 2014.

Fischbach,, J.R., Lempert, R.J., Molina-Perez, E., Tariq, A.A., Finucane, M.L., Hoss, F.: Managing water quality in the face of uncertainty: A robust decision making demonstration

674 for EPA's national water program, Santa Monica, CA: RAND Corporation,
675 http://www.rand.org/pubs/research_reports/RR720.html. Also available in print form, 2015.
676
677 Fleitmann, D., Burns, S.J., Mudelsee, M., Neff, U., Kramers, J., Mangini, A., Matter, A., 2003a.
678 Holocene forcing of the Indian monsoon recorded in a stalagmite from Southern Oman,
679 Science, 300, 1737–1739.
680
681 Folland, C. K., Parker, D. E and Palmer, T. N.: Sahel rainfall and worldwide sea temperatures
682 1901–85, Nature, 320, 602–607, 1986.
683
684 Frierson, D. M. W. and Hwang, Y-T. Extratropical influence on ITCZ shifts in slab ocean
685 simulation of global warming, J. Clim. 25, 720–733, 2012.
686
687 Fuss S., Canadell J.G., Peters G.P., et al.: Betting on negative emissions. Nat Clim Chang 4:
688 850–853, 2014.
689
690 Gabriel, C. J. and Robock, A.: Stratospheric geoengineering impacts on El Niño/Southern
691 Oscillation, Atmos. Chem. Phys., 15, 11949-11966, doi:10.5194/acp-15-11949-2015, 2015.
692
693 Haywood, J. M., Jones, A., Bellouin, N. and Stephenson, D.: Asymmetric forcing from
694 stratospheric aerosols impacts Sahelian rainfall, Nat. Clim. Change, 3(7), 660–665,
695 doi:10.1038/nclimate1857, 2013.
696
697 Held, I. M. and Soden, B. J.: Robust responses of the hydrological cycle to global warming, J.
698 Climate, 19, 5686–5699, 2006.
699
700 Hurley, J. V. and Boos, W. R.: Interannual variability of monsoon precipitation and local
701 subcloud equivalent potential temperature. J. Climate, 26, 9507–9527, 2013.
702
703 Hwang, Y.-T., Frierson, D. M. W. and Kang, S. M.: Anthropogenic sulfate aerosol and the
704 southward shift of tropical precipitation in the late 20th century, Geophys. Res. Lett., 40,
705 doi:10.1002/grl.50502, 2013.
706
707 IPCC: Summary for Policymakers, in: Climate Change 2013: The Physical Science Basis.
708 Contribution of Working Group I to the Fifth Assessment Report of the Intergovernmental
709 Panel on Climate Change, edited by: Stocker, T. F., Qin, D., Plattner, G.-K., Tignor, M.,
710 Allen, S. K., Boschung, J., Nauels, A., Xia, Y., Bex, V., and Midgley, P. M., Cambridge
711 University Press, Cambridge, UK and New York, NY, USA, 2013.
712
713 Irvine, P. J., Ridgwell, A. and Lunt, D. J.: Climatic effects of surface albedo geoengineering, J.
714 Geophys. Res., 116, D24112, doi:10.1029/2011JD016281, 2011.
715
716 Kang, S. M., Held, I. M., Frierson, D. M. W and Zhao, M.: The response of the ITCZ to
717 extratropical thermal forcing: Idealized slab-ocean experiments with a GCM, J.
718 Climate, 21, 3521–3532, 2008.
719

720 Keith, D. W., Duren, R. and MacMartin, D.G.: Field experiments on solar geoengineering: report
721 of a workshop exploring a representative research portfolio. Philosophical Transactions of
722 the Royal Society A., 372-20140175, 2014.
723
724 Kravitz, B., Robock, A., Boucher, O., Schmidt, H., Taylor, K., Stenchikov, G. and Schulz, M.:
725 The geoengineering model intercomparison project (GeoMIP), Atm. Sci. Lett., 12, 162-167,
726 doi: 10.1002/asl.316. 201, 2011.
727
728 Kravitz, B., Rasch, P.J., Forster, P.M., Andrews, T., Cole, J.N.S., Irvine, P.J., Ji, D.,
729 Kristjánsson, J.-E., Moore, J.C., Muri, H., Niemeier, U., Robock, A., Singh, B., Tilmes, S.,
730 Watanabe, S. and Yoon, J.-H.: An energetic perspective on hydrological cycle changes in the
731 Geoengineering Model Intercomparison Project (GeoMIP), J. Geophysical Research, 118,
732 13,087-13,102, doi:10.1002/2013JD020502, 2013.
733
734 Kravitz, B., Robock, A., Tilmes, S., Boucher, O., English, J. M., Irvine, P. J., Jones, A.,
735 Lawrence, M. G., MacCracken, M., Muri, H., Moore, J. C., Niemeier, U., Phipps, S. J.,
736 Sillmann, J., Storelvmo, T., Wang, H., and Watanabe, S.: The Geoengineering Model
737 Intercomparison Project Phase 6 (GeoMIP6): simulation design and preliminary results,
738 Geosci. Model Dev. Discuss., 8, 4697–4736, doi:10.5194/gmdd-8-4697-2015, 2015.
739
740 Jones A., Haywood, J. and Boucher, O.: Climate impacts of geoengineering marine
741 stratocumulus clouds, J. Geophys. Res., 114, D10106, doi:10.1029/2008JD011450, 2009.
742
743 Kay J.E., Wall C., Yettella V., Medeiros B., Hannay C., Caldwell P. and Bitz C.: Global
744 climate impacts of fixing the Southern Ocean shortwave radiation bias in the community
745 earth system model (CESM), J Climate, doi:10.1175/JCLI-D-15-0358, 2016.
746
747 Lamarque, J.-F., Emmons, L. K., Hess, P. G., Kinnison, D. E., Tilmes, S., Vitt, F., Heald, C. L.,
748 Holland, E. A., Lauritzen, P. H., Neu, J., Orlando, J. J., Rasch, P. J., and Tyndall, G. K.:
749 CAM-chem: description and evaluation of interactive atmospheric chemistry in the
750 Community Earth System Model, Geosci. Model Dev., 5, 369–411, doi:10.5194/gmd-5-369-
751 2012, 2012.
752
753 Latham, J., Bower, K., Choularton, T., Coe, H., Connoly, P., Cooper, G., Craft, T., Foster, J.,
754 Gadian, A., Galbraith, L., Iacovides, H., Johnston, D., Launder, B., Leslie, B., Meyer, J.,
755 Neukermans, A., Ormond, B., Parkes, B., Rasch, P., Rush, J., Salter, S., Stevenson, T.,
756 Wang, H., Wang, Q., and Wood, R.: Marine cloud brightening, Phil. Trans. R. Soc. A, 370,
757 4217–4262, doi:10.1098/rsta.2012.0086, 2012.
758
759 Manabe, S. and Stouffer, R. J.: Sensitivity of a global climate model to an increase of CO_2
760 concentration in the atmosphere. J. Geophys. Res. 85, 5529–5554, 1980.
761
762 Meehl, G. A., Arblaster, J. M., Caron, J. M., Annamalai, H., Jochum, M., Chakraborty, A., and
763 Murtugudde, R.: Monsoon regimes and processes in CCSM4. Part I: The Asian-Australian
764 Monsoon, J. Climate, 25, 2583–2608, 2012.
765

766 Meinshausen, M., Smith, S. J., Calvin, K., Daniel, J. S., Kainuma, M. L. T., Lamarque, J.-F.,
767 Matsumoto, K., Montzka, S. A., Raper, S. C. B., Riahi, K., Thomason, A., Velders, G. J. M.,
768 and van Vuuren, D. P. P.: The RCP greenhouse gas concentrations and their extension from
769 1765 to 2300, Climatic Change, 109, 213– 241, doi:10.1007/s10584-011-0156-z, 2011.
770
771 Miller, K. G., Kopp, R.E., Horton, B.P., Browning, J.V. and Kemp, A.C.: A geological
772 perspective on sea-level rise and its impacts along the U.S. mid-Atlantic coast. Earth's Future
773 1, 3–18. doi: 10.1002/ 2013EF000135, 2013.
774
775 Neely III, R. R., Conley, A. J., Vitt, F., and Lamarque, J.-F.: A consistent prescription of
776 stratospheric aerosol for both radiation and chemistry in the Community Earth System Model
777 (CESM1), Geosci. Model Dev., 9, 2459-2470, doi:10.5194/gmd-9-2459, 2016.
778
779 Poore, R. Z., Quinn, T.M. and Verardo, S.: Century-scale movement of the Atlantic Intertropical
780 Convergence Zone linked to solar variability, Geophysical Research Letters, 31, L12214,
781 doi: 10.1029/2004GL019940, 2004.
782
783 Rasch P. J., Latham, J. and Chen, C.C.: Geoengineering by cloud seeding: influence on sea ice
784 and climate system, Environmental Research Letters, 4, 45-112. doi:10.1088/1748-
785 9326/4/4/045112, 2009.
786
787 Reason, C. J. C.: Subtropical Indian Ocean SST dipole events and southern African
788 rainfall, Geophys. Res. Lett., 28, 2225-2228, 10.1029/2000GL012735, 2001.
789
790 Robock, A., L. Oman, L., and Stenchikov, G.: Regional climate responses to geoengineering
791 with tropical and Arctic SO_2 injections, Journal of Geophysical Research, 113, D16101, doi:
792 10.1029/2008JD010050, 2008.
793
794 Robock, A.: 20 reasons why geoengineering may be a bad idea, Bull. Atomic Sci., 64, 14–18,
795 doi:10.2968/064002006, 2008.
796
797 Robock, A.: Bubble, bubble, toil and trouble. An editorial comment. Climatic Change, 105, 383-
798 385, doi:10.1007/s10584-010-0017-1, 2011.
799
800 Robock, A.: Stratospheric aerosol geoengineering, Issues Env. Sci. Tech. (special issue
801 "Geoengineering of the Climate System"), 38, 162-185, 2014.
802
803 Sanderson B.M., O'Neill B., Tebaldi C.: What would it take to achieve the Paris temperature
804 targets? Geophys Res Lett, 1, 10., doi:10.1002/2016GL069563, 2016.
805
806 Seitz, R.: Bright water: hydrosols, water conservation and climate change. Climatic Change,
807 105, 365–381, 2010.
808
809 Siegenthaler, U., Stocker, T. F., Monnin, E., Luthi, D., Schwander J., Stauffer, B., Raynaud, D.,
810 Barnola, J. M., Fischer, H., Masson, Delmotte, V., and Jouzel, J.: Stable carbon cycle-climate
811 relationship during the late Pleistocene, Science, 310, 1313–1317, 2005.

812
813 Suzuki, R., Behera, S.K., Iizuka, S. and Yamagata, T.: The Indian Ocean subtropical dipole
814 simulated using a CGCM, J. Geo. Res. 109, doi:10.1029/2003JC001974, 2004.
815
816 Taylor, K. E., Stouffer, R. J., and Meehl, G. A.: An overview of CMIP5 and the experiment
817 design, B. Am. Meteorol. Soc., 93, 485–498, doi:10.1175/BAMS-D-11-00094.1, 2012.
818
819 Tilmes, S., Fasullo, J., Lamarque, J.-F., Marsh, D. R., Mills, M., Alterskjaer, K., Muri, H.,
820 Kristjánsson, J. E., Boucher, O., Schulz, M., Cole, J. N. S., Curry, C. L., Jones, A., Haywood,
821 J., Irvine, P. J., Ji, D., Moore, J. C., Karam, D. B., Kravitz, B., Rasch, P. J., Singh, B., Yoon,
822 J.-H., Niemeier, U., Schmidt, H., Robock, A., Yang, S., and Watanabe, S.: The hydrological
823 impact of geoengineering in the Geoengineering Model Intercomparison Project (GeoMIP),
824 J. Geophys. Res.-Atmos, 118, 11036–11058, doi:10.1002/jgrd.50868, 2013.
825
826 Tilmes, S., Mills, M. J., Niemeier, U., Schmidt, H., Robock, A., Kravitz, B., Lamarque, J.-F.,
827 Pitari, G., and English, J. M.: A new Geoengineering Model Intercomparison Project
828 (GeoMIP) experiment designed for climate and chemistry models, Geosci. Model Dev., 8,
829 43-49, doi:10.5194/gmd-8-43-2015, 2015.
830 .
831 Tilmes, S., Lamarque, J.-F., Emmons, L. K., Kinnison, D. E., Marsh, D., Garcia, R. R., Smith, A.
832 K., Neely, R. R., Conley, A., Vitt, F., Val Martin, M., Tanimoto, H., Simpson, I., Blake, D.
833 R., and Blake, N.: Representation of the Community Earth System Model (CESM1) CAM4-
834 chem within the Chemistry-Climate Model Initiative (CCMI), Geosci. Model Dev., 9, 1853-
835 1890, doi:10.5194/gmd-9-1853-2016, 2016.
836
837 Trenberth, K. E., and Dai, A.: Effects of Mount Pinatubo volcanic eruption on the hydrological
838 cycle as an analog of geoengineering, Geophys. Res. Lett., 34, L15702,
839 doi:10.1029/2007GL030524, 2007.
840
841 Xia, L., Robock, A., Tilmes, S., and Neely III, R. R.: Stratospheric sulfate geoengineering could
842 enhance the terrestrial photosynthesis rate, Atmos. Chem. Phys., 16, 1479-1489,
843 doi:10.5194/acp-16-1479-2016, 2016.
844
845 Xie, S-P. and Philander, S. G. H. A coupled ocean-atmosphere model of relevance to the ITCZ in
846 the eastern Pacific, Tellus, 46A, 340–350, 1994.
847

Atmos. Chem. Phys. Discuss., doi:10.5194/acp-2016-849, 2016
Manuscript under review for journal Atmos. Chem. Phys.
Published: 5 October 2016

Atmospheric Chemistry and Physics Discussions

848 **Table 1.** Changes in temperature and precipitation in G4Foam relative to both G4SSA and
849 RCP6.0, for the entire globe and for the Tropics (20°S-20°N) annually and in Northern
850 Hemisphere summer, for the 40-year period beginning 10 years after the start of climate
851 engineering.
852

Global, 2030-2069	**G4Foam – G4SSA (% change)**	**G4Foam – RCP6.0 (% change)**
Precipitation (mm/day)	+0.02 (+0.61)	-0.06 (-1.98)
Land precipitation (mm/day)	+0.07 (+3.19)	+0.01 (+0.32)
Ocean precipitation (mm/day)	–0.01 (–0.36)	–0.08 (–2.57)
Temperature (K)	+0.27	–0.53
Land temperature (K)	+0.63	–0.44
Global, 2030-2069, June-July-August		
Precipitation (mm/day)	+0.02 (+0.70)	-0.05 (-1.85)
Land precipitation (mm/day)	+0.08 (+3.35)	+0.02 (+0.70)
Ocean precipitation (mm/day)	+0.01 (-0.29)	–0.08 (–2.51)
Temperature (K)	+0.32	–0.60
Land temperature (K)	+0.71	–0.53
Tropical, 2030-2069		
Precipitation (mm/day)	+0.06 (+1.59)	–0.03 (–1.06)
Land precipitation (mm/day)	+0.16 (+3.93)	+0.07 (+1.43)
Ocean precipitation (mm/day)	+0.03 (+0.77)	–0.07 (–1.92)
Temperature (K)	+0.21	–0.60
Land temperature (K)	+0.43	–0.61
Tropical, 2030-2069, June-July-August		
Precipitation (mm/day)	+0.06 (+1.52)	–0.03 (–0.84)
Land precipitation (mm/day)	+0.16 (+4.66)	+0.07 (+2.02)
Ocean precipitation (mm/day)	+0.03 (+0.67)	–0.06 (–1.61)
Temperature (K)	+0.18	–0.61
Land temperature (K)	+0.37	–0.70

853

Atmos. Chem. Phys. Discuss., doi:10.5194/acp-2016-849, 2016
Manuscript under review for journal Atmos. Chem. Phys.
Published: 5 October 2016

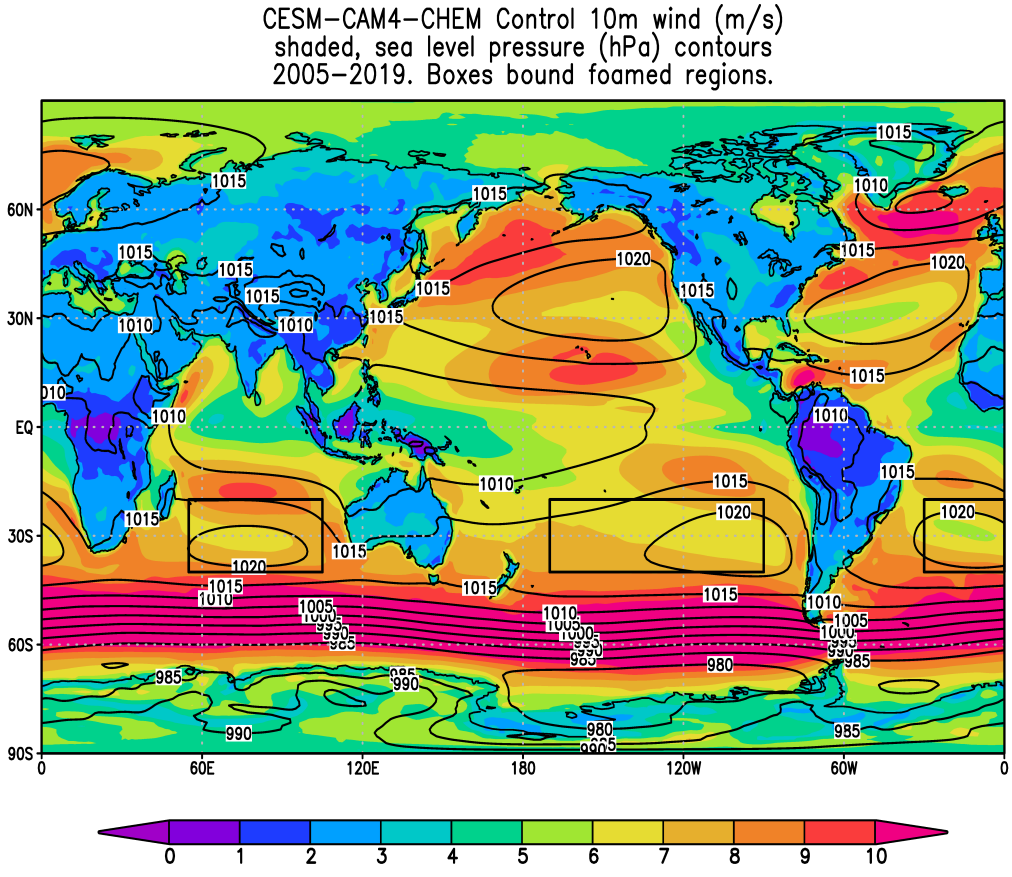

Figure 1. Applied forcing and global mean temperature response. Ocean albedo changed from daily average of 0.0]6 to a fixed value of 0.15 over "foam regions," 20°N-20°S, 90°W-170°W (South Pacific), 20°N-20°S, 30°W-0°E (South Atlantic) and 20°N-20°S, 55°E-105°E (South Indian). Each "foamed" region is outlined in black. Control run sea level pressure (mb) is shown with contours and 10-m winds (m/s) are shaded.

Atmos. Chem. Phys. Discuss., doi:10.5194/acp-2016-849, 2016
Manuscript under review for journal Atmos. Chem. Phys.
Published: 5 October 2016

Atmospheric Chemistry and Physics Discussions

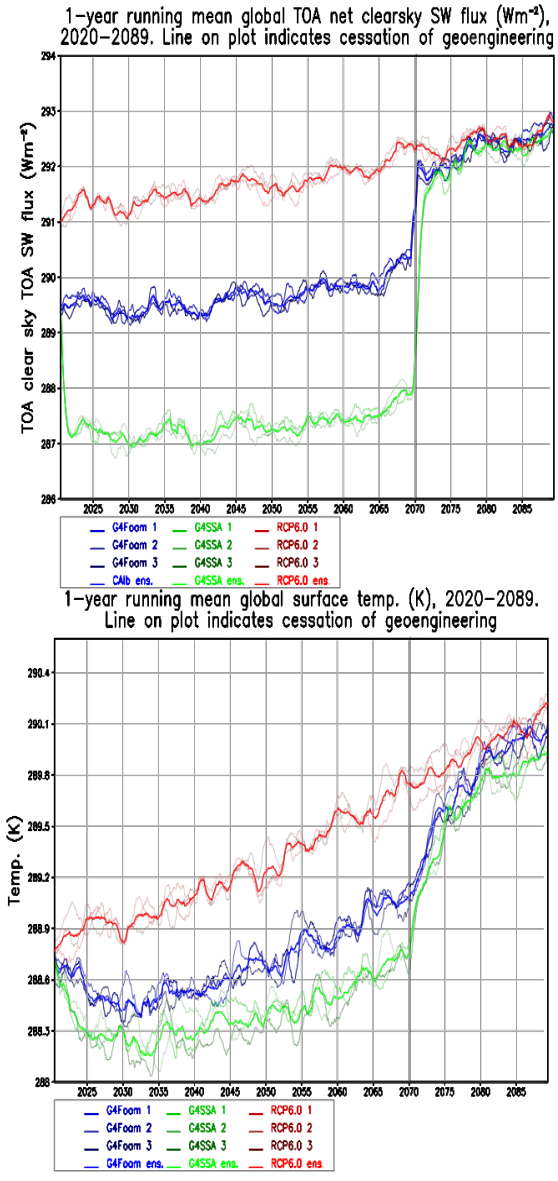

Figure 2. (a) Net clear sky SW flux at top of atmosphere, which includes the effects of changes in radiation caused by changes in ocean surface albedo or land albedo (ice and snow), as well as stratospheric aerosols (stratospheric geoengineering) and (b) Time series of global mean temperature. In G4Foam, temperature is more than twice as sensitive to ocean albedo forcing as it is to stratospheric geoengineering, as applied in G4SSA, albeit with very different latitudinal distributions of temperature changes. Each ensemble member and the ensemble mean are shown for each forcing.

Atmos. Chem. Phys. Discuss., doi:10.5194/acp-2016-849, 2016
Manuscript under review for journal Atmos. Chem. Phys.
Published: 5 October 2016

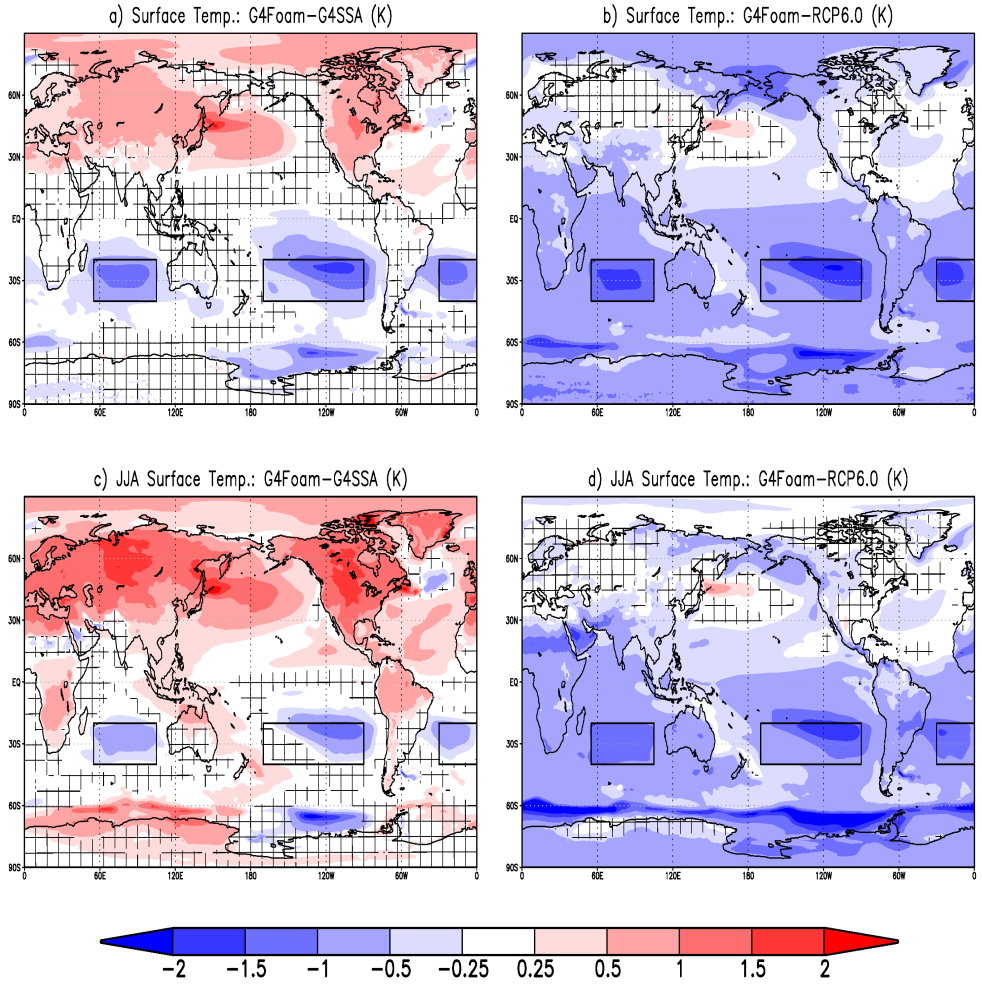

Figure 3. 2030-2069 surface temperature differences (K) between G4Foam and (a) G4SSA, (b) RCP6.0, (c) G4SSA during JJA, and (d) RCP6.0 during JJA. Hatched regions are areas with $p >$ 0.05 (where changes are not statistically significant based on a paired *t*-test). Black boxes enclose foamed regions.

Atmos. Chem. Phys. Discuss., doi:10.5194/acp-2016-849, 2016
Manuscript under review for journal Atmos. Chem. Phys.
Published: 5 October 2016

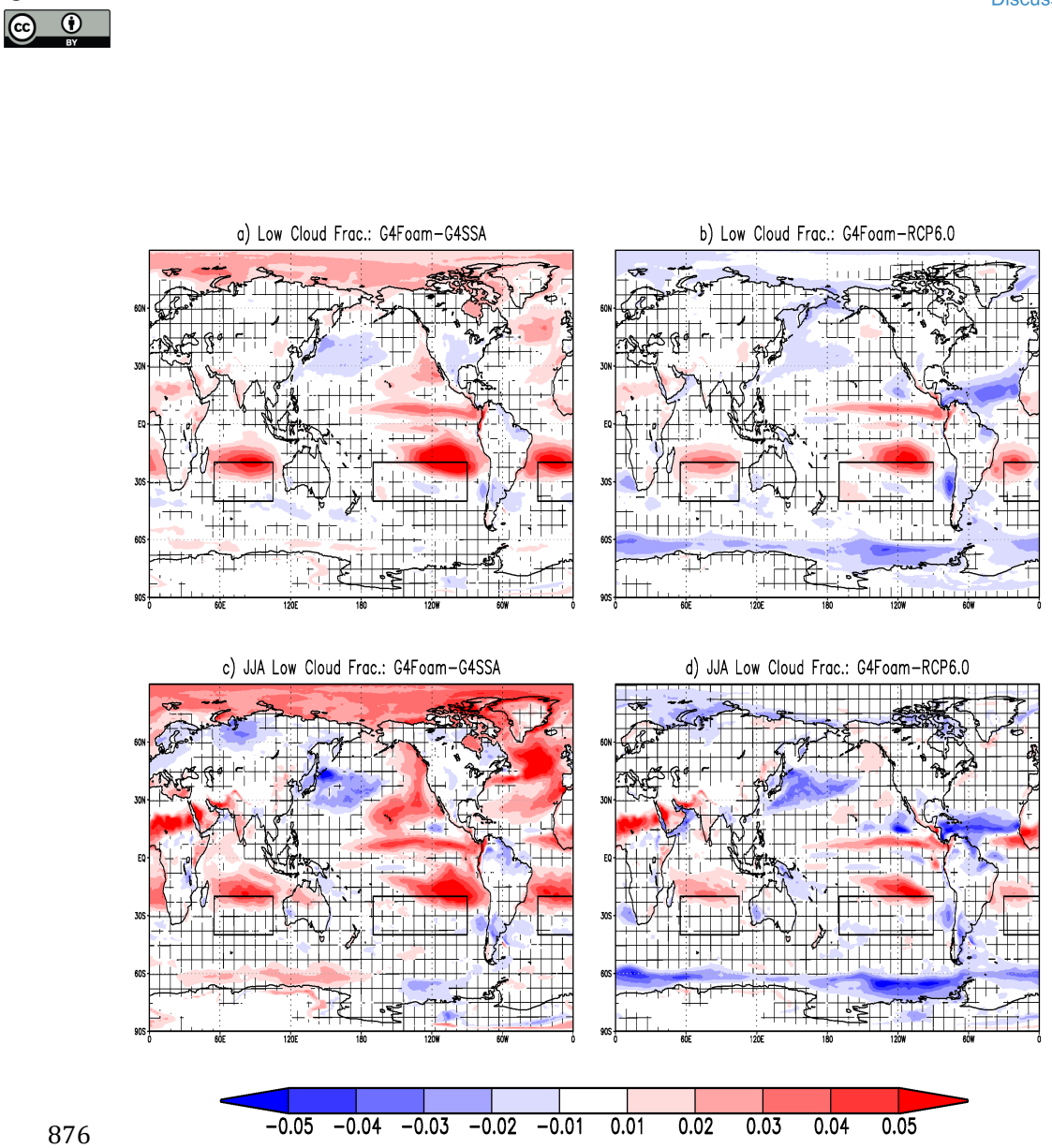

Figure 4. 2030-2069 low cloud fraction difference (unitless) between G4Foam and (a) G4SSA, (b) RCP6.0, (c) G4SSA during JJA, and (d) RCP6.0 during JJA. Hatched regions are areas with $p > 0.05$ (where changes are not statistically significant based on a paired *t*-test). Black boxes enclose foamed regions.

Atmos. Chem. Phys. Discuss., doi:10.5194/acp-2016-849, 2016
Manuscript under review for journal Atmos. Chem. Phys.
Published: 5 October 2016

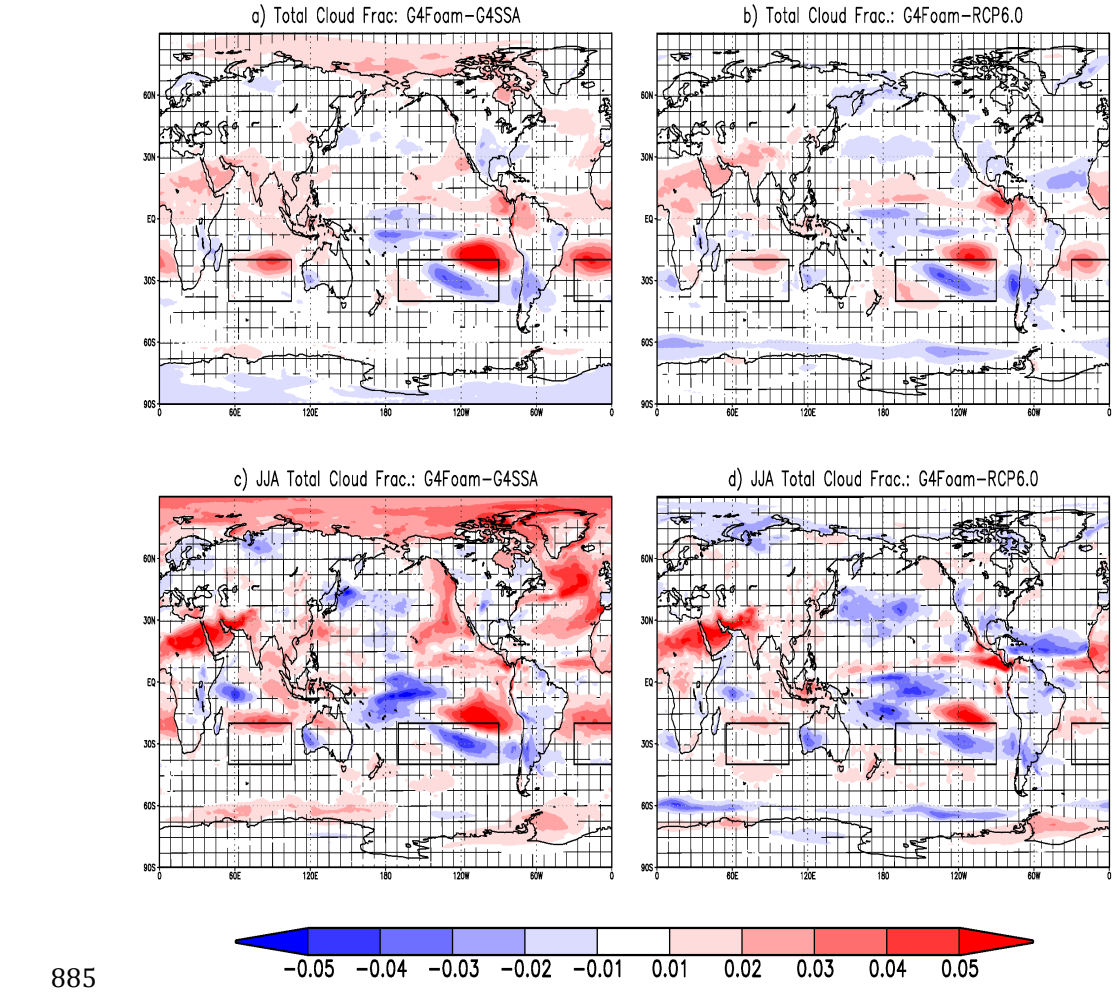

Figure 5. 2030-2069 total cloud fraction difference (unitless) between G4Foam and (a) G4SSA, (b) RCP6.0, (c) G4SSA during JJA and (d) RCP6.0 during JJA. Hatched regions are areas with $p > 0.05$ (where changes are not statistically significant based on a paired *t*-test). Black boxes enclose foamed regions.

Atmos. Chem. Phys. Discuss., doi:10.5194/acp-2016-849, 2016
Manuscript under review for journal Atmos. Chem. Phys.
Published: 5 October 2016

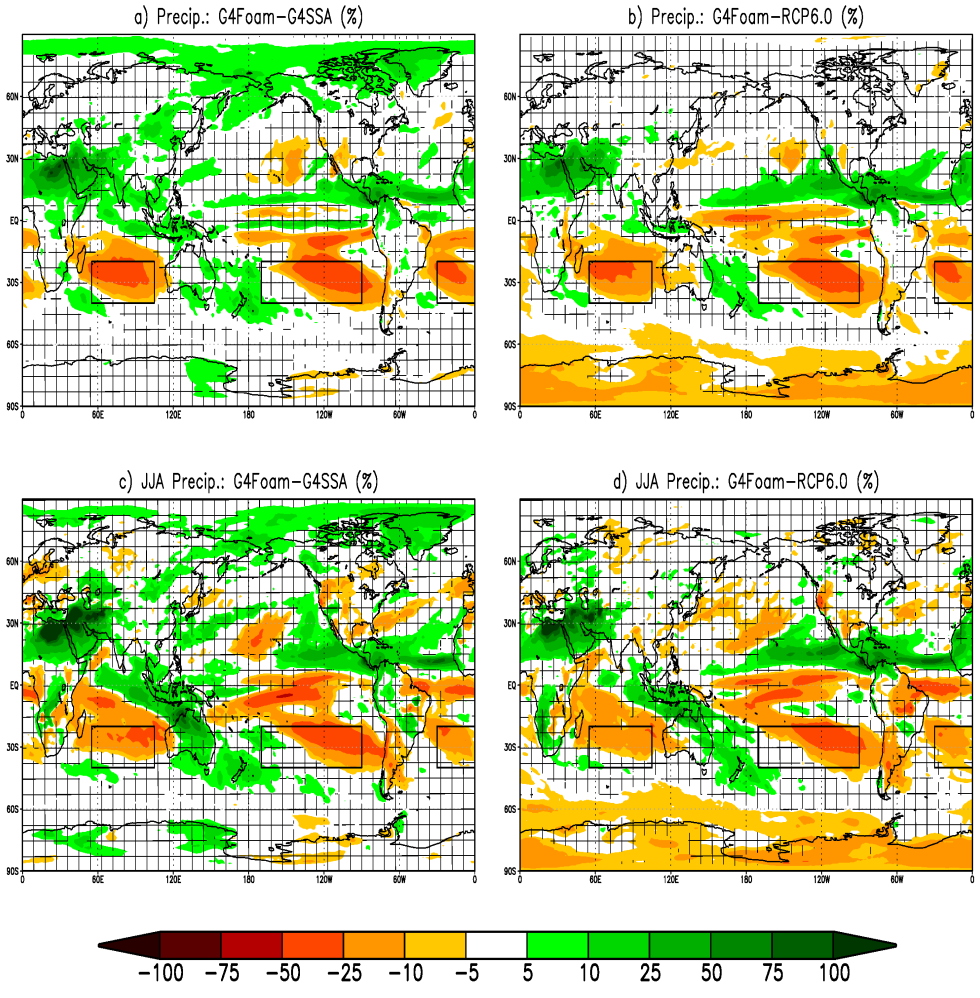

Figure 6. 2030-2069 precipitation difference (%) between G4Foam and (a) G4SSA, (b) RCP6.0, (c) G4SSA during JJA and (d) RCP6.0 during JJA. Hatched regions are areas with $p >$ 0.05 (where changes are not statistically significant based on a paired *t*-test). Black boxes enclose foamed regions.

Atmos. Chem. Phys. Discuss., doi:10.5194/acp-2016-849, 2016
Manuscript under review for journal Atmos. Chem. Phys.
Published: 5 October 2016

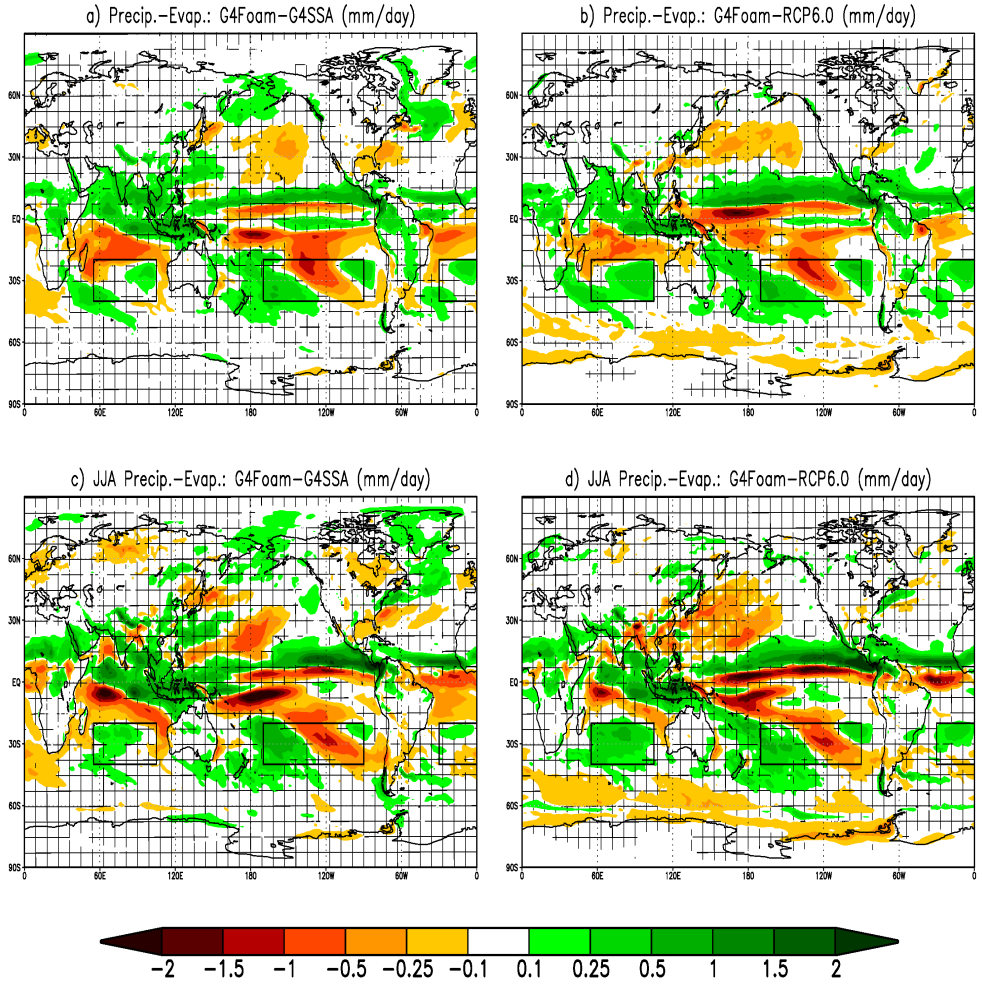

Figure 7. 2030-2069 precipitation minus evaporation difference (mm/day) between G4Foam and (a) G4SSA, (b) RCP6.0, (c) G4SSA during JJA and (d) RCP6.0 during JJA. Hatched regions are areas with $p > 0.05$ (where changes are not statistically significant based on a paired *t*-test). Black boxes enclose foamed regions.

Atmos. Chem. Phys. Discuss., doi:10.5194/acp-2016-849, 2016
Manuscript under review for journal Atmos. Chem. Phys.
Published: 5 October 2016

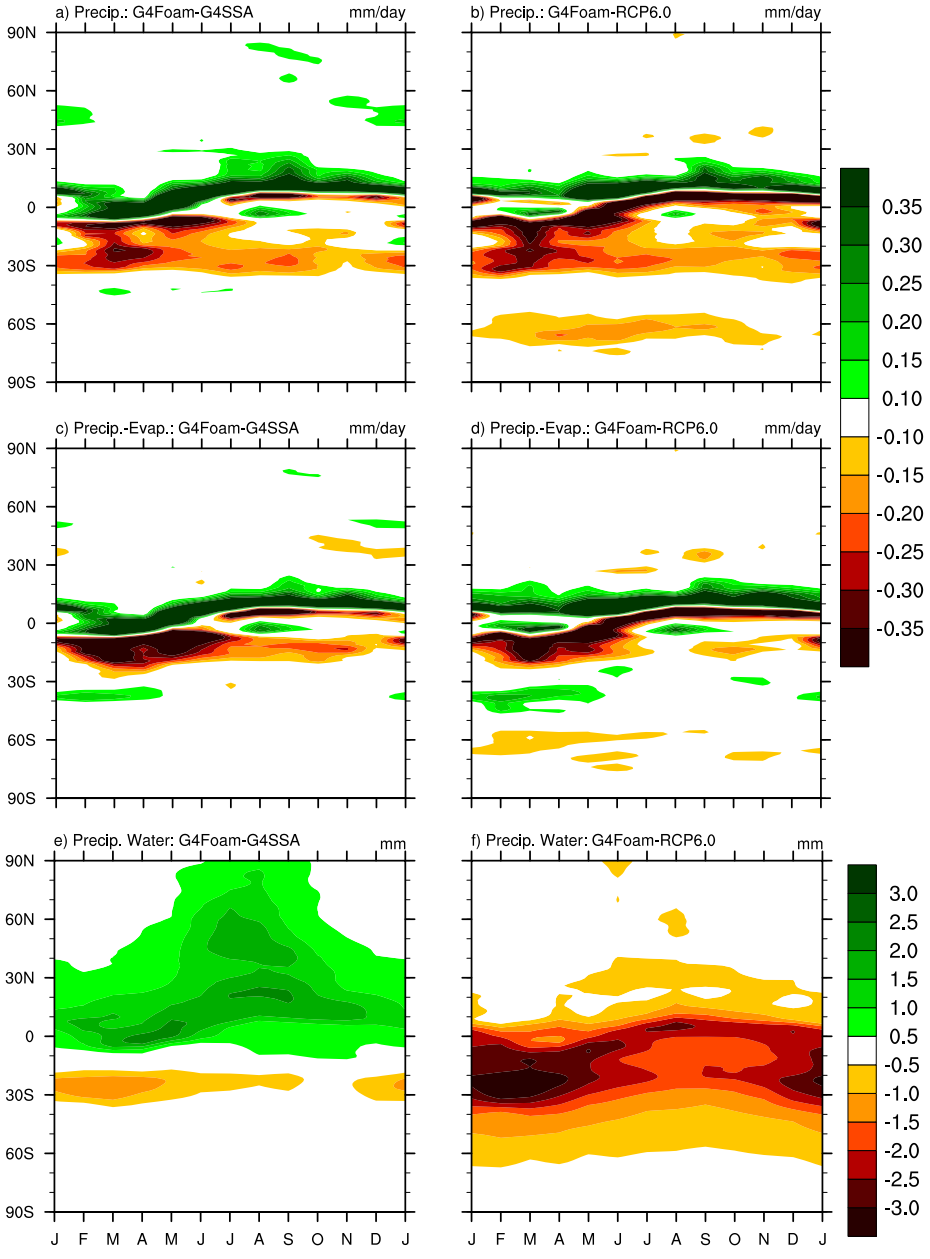

Figure 8. 2030-2069 monthly mean annual cycle of zonal mean precipitation (mm/day) for (a) G4Foam minus G4SSA and (b) G4Foam minus RCP6.0, precipitation minus evaporation (mm/day) for (c) G4Foam minus G4SSA and (d) G4Foam minus RCP6.0, and total precipitable water (mm) for (e) G4Foam minus G4SSA and (f) G4Foam minus RCP6.0.

Atmos. Chem. Phys. Discuss., doi:10.5194/acp-2016-849, 2016
Manuscript under review for journal Atmos. Chem. Phys.
Published: 5 October 2016

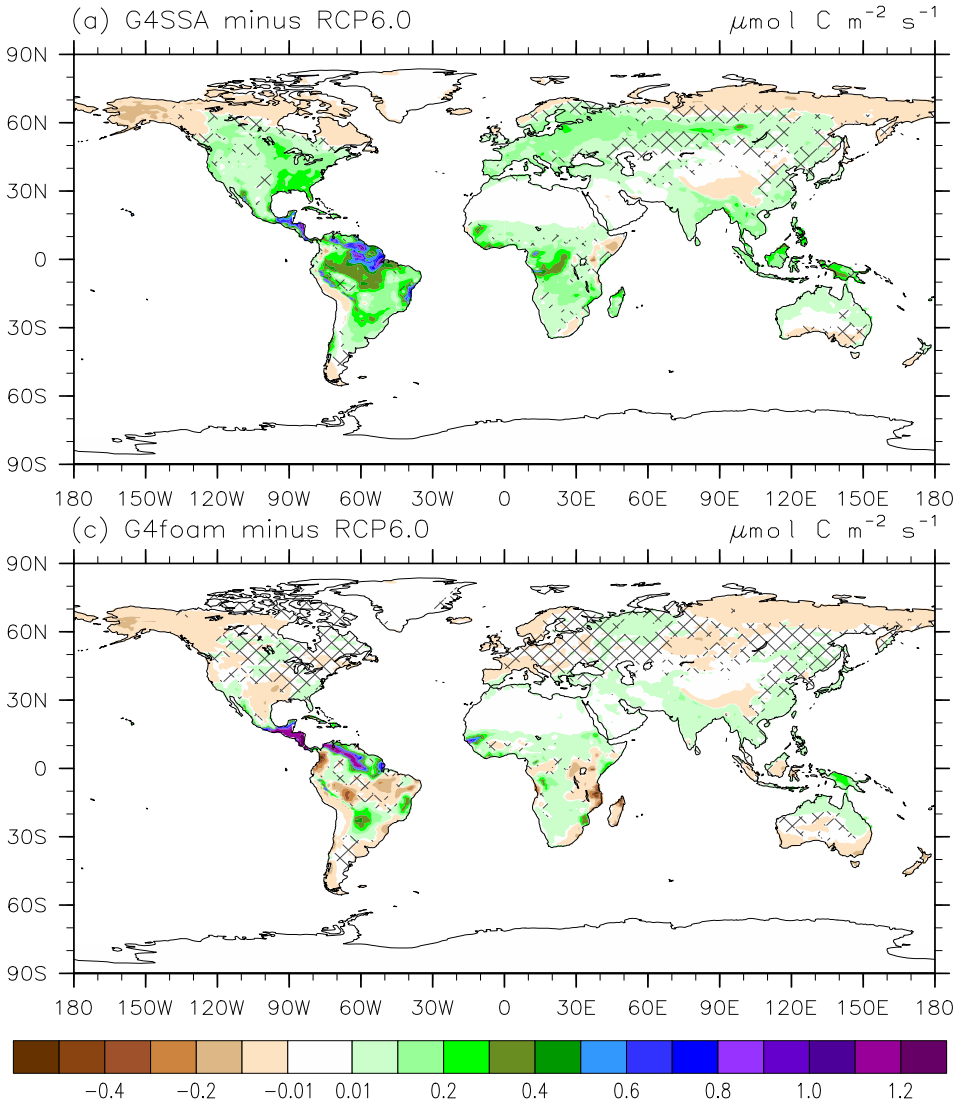

Figure 9. (a) Photosynthesis rate differences between G4SSA and RCP6.0 during years 2030–2069 (sulfate injection period, excluding the first 10 years) (Fig. 4a from Xia et al., 2016). (b) Photosynthesis rate anomaly between G4Foam and RCP6.0 during years 2030–2069 of solar reduction. Hatched regions are areas with $p > 0.05$ (where changes are not statistically significant based on a paired t test).